

1   **Title : Is adaptation limited by mutation? A timescale-dependent effect of genetic**  
2   **diversity on the adaptive substitution rate in animals**

3   **Authors :** Rousselle M<sup>1</sup>, Simion P<sup>1,2</sup>, Tilak MK<sup>1</sup>, Figuet E<sup>1</sup>, Nabholz B<sup>1</sup>, Galtier N<sup>1</sup>.

4   <sup>1</sup>ISEM, Univ. Montpellier, CNRS, EPHE, IRD, Montpellier, France.

5   <sup>2</sup>LEGE, Department of Biology, University of Namur, 5000 Namur, Belgium.

6   **Corresponding author:** Marjolaine Rousselle

7   marjolaine.rousselle@umontpellier.fr

## 8 ABSTRACT

9 Whether adaptation is limited by the beneficial mutation supply is a long-standing question of  
10 evolutionary genetics, which is more generally related to the determination of the adaptive  
11 substitution rate and its relationship with the effective population size  $N_e$ . Empirical evidence  
12 reported so far is equivocal, with some but not all studies supporting a higher adaptive substitution  
13 rate in large- $N_e$  than in small- $N_e$  species.

14 We gathered coding sequence polymorphism data and estimated the adaptive amino-acid  
15 substitution rate  $\omega_a$ , in 50 species from ten distant groups of animals with markedly different  
16 population mutation rate  $\theta$ . We reveal the existence of a complex, timescale dependent relationship  
17 between species adaptive substitution rate and genetic diversity. We find a positive relationship  
18 between  $\omega_a$  and  $\theta$  among closely related species, indicating that adaptation is indeed limited by the  
19 mutation supply, but this was only true in relatively low- $\theta$  taxa. In contrast, we uncover a weak  
20 negative correlation between  $\omega_a$  and  $\theta$  at a larger taxonomic scale. This result is consistent with  
21 Fisher's geometrical model predictions and suggests that the proportion of beneficial mutations  
22 scales negatively with species' long-term  $N_e$ .

23 **Key words:** adaptive substitution rate, beneficial mutations, effective population size, Mc-Donald  
24 and Kreitman, animals.

## 25 INTRODUCTION

26 It is widely recognized that adaptation is more efficient in large populations. Firstly, large  
27 populations produce a greater number of mutants per generation than small ones, and for this reason  
28 are more likely to find the alleles required for adaptation, if missing from the gene pool. Secondly,  
29 large populations tend to be genetically more diverse and thus more likely to carry the alleles  
30 needed to respond to environmental changes (1). Lastly, the fixation probability of beneficial  
31 mutations is higher in large than in small populations due to the weaker effect of genetic drift in the  
32 former. So, whether it be from standing variation or *de novo* mutations, one would expect to  
33 observe a higher rate of accumulation of adaptive changes, on average, in large than in small  
34 populations (2). Under a simple population genetic model, in a population of effective size  $N_e$ ,  
35 mutations of selection coefficient  $s >> 1/N_e$  should accumulate at rate  $\sim 4N_e\mu_a s$  if  $s$  is small, where  $\mu_a$   
36 is the adaptive mutation rate – i.e., the adaptive substitution rate should scale linearly with  $N_e\mu_a$   
37 (where  $\mu$  is the total mutation rate) (3).

38 This rationale implicitly assumes that the rate of adaptation is limited by the supply of new  
39 mutations, i.e., the population mutation rate  $\theta = 4N_e\mu$  (4). It might be, however, that the amount of  
40 genetic diversity available in all or most existing populations is sufficient for adaptation, and/or that  
41 the ability to adapt to environmental changes is determined in the first place by factors independent  
42 from the effective population size, such as the magnitude or frequency of perturbations, the finite  
43 set of possible genotypes an organism could reach, or the ability of populations to combine  
44 favorable alleles across loci via recombination (5–10). Finally, this rationale makes the assumption  
45 of a constant distribution of the fitness effect (DFE) across species, whereas it has been suggested  
46 that the adaptive mutation rate,  $\mu_a$ , might be negatively correlated with  $N_e$ , which further  
47 complicates the situation. This is because small populations tend to accumulate deleterious  
48 mutations, and the resulting load could offer the opportunity for adaptive, compensatory mutations  
49 to arise and spread irrespective of environmental perturbations (9). Theoretical models can therefore  
50 predict a positive, negative, or lack of relationship between the population size and the adaptive  
51 substitution rate, depending on the underlying assumptions.

52 Molecular data offer an unique opportunity to empirically evaluate the correlation between the  
53 adaptive substitution rate and  $\theta$ , and thus to test whether adaptation is actually limited by mutation.  
54 More efficient adaptation in large populations should be reflected by an increased protein

55 evolutionary rate, which can be estimated from coding sequence alignments. The ratio of non-  
56 synonymous (i.e. amino-acid changing, dN) to synonymous (i.e. amino-acid conservative, dS)  
57 substitution rates, often called  $\omega$ , is a measure of the protein evolutionary rate that controls for the  
58 effects of the divergence time and mutation rate. However,  $\omega$  is influenced by adaptation but also  
59 by the strength and efficiency of purifying selection against deleterious alleles. To account for this,  
60 McDonald and Kreitman (1991, MK) (10) suggested including within-species polymorphism in the  
61 analysis. Adaptive mutations are expected to contribute negligibly to the pool of segregating alleles.  
62 The ratio of non-synonymous to synonymous polymorphism, therefore, provides an estimator of the  
63 expected  $\omega$  under neutrality, i.e., in absence of adaptation, called  $\omega_{na}$  (for non-adaptive). Subtracting  
64 the neutral expectation  $\omega_{na}$  from the observed  $\omega$  provides an estimator of the adaptive rate,  $\omega_a$ , and  
65 the proportion of adaptive substitutions,  $\alpha$  (11).

66 Subsequent improvements in the MK method were intended to account for a number of factors that  
67 could potentially confound the estimation of  $\omega_{na}$ , including the prevalence of slightly deleterious  
68 segregating alleles and recent demographic effects (14–21). Improved methods explicitly model the  
69 DFE of non-synonymous mutations, while taking information not only from the number of  
70 synonymous and non-synonymous single nucleotide polymorphisms (SNPs), but also from the  
71 distribution of allele frequencies across SNPs – so-called site frequency spectra (SFS). The  $\omega_a$   
72 statistics has a high sampling variance (22) and its estimation can be biased by various factors, such  
73 as a fluctuating population size (12,23,24) and GC-biased gene conversion (25–27). In particular,  
74 one key assumption of the MK approach is that the long-term  $N_e$ , which determines  $\omega$ , is equal to  
75 the short-term  $N_e$  and can therefore be estimated from polymorphism data. It appears unlikely that  
76 this is generally true, and ancient fluctuations in  $N_e$  could in principle fault the MK rationale  
77 (12,23,24). Eyre-Walker (24) theoretically considered the problem of a single ancient change in  $N_e$   
78 and showed that an expansion in population size, even if old, could lead to overestimation of the  
79 adaptive substitution rate. This bias could create spurious positive correlation between  $\omega_a$  and  $N_e$ ,  
80 which should be kept in mind when interpreting this type of estimate.

81 The first applications of the MK method to large-scale data sets indicated that the adaptive rate is  
82 higher in *Drosophila* than in humans (11,13,14). This is consistent with the prediction of more  
83 efficient adaptation in large populations and with the hypothesis that mutation limits adaptation.  
84 These studies were, however, focused on the  $\alpha = \omega_a / (\omega_a + \omega_{na})$  statistics, i.e., the proportion of amino-  
85 acid substitutions that result from adaptation.  $\alpha$  is influenced by  $\omega_{na}$  as well as  $\omega_a$ , and a lower  $\alpha$  in

86 humans than in *Drosophila* might mainly reflect a higher rate of non-adaptive amino-acid  
87 substitution in the former. Indeed, purifying selection against deleterious mutations is likely less  
88 effective in small populations due to increased genetic drift (28). Comparative studies focused on  $\omega_a$   
89 have only revealed tenuous positive effects of  $\theta$  on the adaptive rate in mammals, flies and plants  
90 (29–31). The largest scale analysis of this sort used 44 pairs of non-model species of animals  
91 occupying a wide range of  $\theta$  (18). This latter study reported a significantly positive relationship  
92 between  $\theta$ -related life history traits and  $\alpha$ , consistent with previous literature, but this was entirely  
93 due to the non-adaptive component. Galtier (18) failed to detect any effect of  $\theta$  on  $\omega_a$ , despite using  
94 various models for the distribution of fitness effects and accounting for a number of potential  
95 confounding factors—. This result did not support the hypothesis that adaptation is limited by  
96 mutation.

97 So, the evidence so far regarding the relationship between the adaptive substitution rate and the  
98 population mutation rate is equivocal. Existing comparative studies have involved distinct  
99 methodological approaches, both in terms of species sampling and adaptive substitution rate  
100 estimation. In particular, these studies were conducted at different evolutionary scales, which might  
101 partially explain their somewhat discordant results. In the short term, an increase in  $N_e$  is expected  
102 to boost the adaptive substitution rate if the mutation supply is limiting. In the long run, differences  
103 in  $N_e$  could also lead to changes in the DFE, and particularly in the proportion of beneficial  
104 mutations, due to the fact that small- $N_e$  species may be pulled away from their fitness optimum via  
105 genetic drift (11,18,32). How these two opposing forces interact and combine to determine the  
106 relationship between  $\omega_a$  and  $\theta$  is still unknown, in the absence of a multi-scale study.

107 In this study, we test the effects of the evolutionary time-scale on the relationship between the  
108 adaptive substitution rate ( $\omega_a$ ) and the population mutation rate ( $\theta$ ). We gathered coding sequence  
109 polymorphism data in 4–6 species from each of ten distant groups of animals with markedly  
110 different  $\theta$ . Our results reveal that the relationship between  $\omega_a$  and  $\theta$  varies depending on the  
111 considered taxonomic scale, i.e. depending on whether we compare closely related species or  
112 distantly related taxa. We report a positive relationship between  $\omega_a$  and  $\theta$  within groups, and the  
113 strength of this relationship weakens as  $\theta$  increases, indicating that adaptation is limited by  
114 beneficial mutations in small- $\theta$  animal species. At a larger taxonomic scale, in contrast, we find a  
115 weak negative correlation between  $\omega_a$  and  $\theta$ , with, for instance, primates and ants showing a higher

116 adaptive substitution rate than mussels and fruit flies. This is in line with the hypothesis that long-  
117 term  $N_e$  influences the DFE, and particularly the proportion of adaptive mutations.

118 **RESULTS**

119 **1. Data sets**

120 We assembled a data set of coding sequence polymorphism in 50 species from ten taxonomic  
121 groups, each group including 4 to 6 closely-related species (**Table S1**). The ten taxa we analyzed  
122 were Catharrhini (Mammalia, hereafter called “primates”), Passeriformes (Aves, hereafter called  
123 “passerines”), Galloanserae (Aves, hereafter called “fowls”), Muroidea (Mammalia, hereafter called  
124 “rodents”), Lumbricidae (Annelida, hereafter called “earth worms”), *Lineus* (Nemertea, hereafter  
125 called “ribbon worms”), *Mytilus* (Mollusca, hereafter called “mussels”), Satyrini (Lepidoptera,  
126 hereafter called “butterflies”), *Formica* (Hymenoptera, hereafter called “ants”), and *Drosophila*  
127 (hereafter called “flies”).

128 Data for five groups (primates, passerines, fowls, rodents and flies) were obtained from public  
129 databases. Data for the other five groups were newly generated via exon capture in a total of 242  
130 individuals from 22 species (**Table 1**) and we obtained sufficient data for 216 of them (~89%). The  
131 average coverage was of 9X in ants, 23X in butterflies, 10X in earth worms, 28X in ribbon worms  
132 and 26X in mussels (average of median coverage per species). The percentage of targeted coding  
133 sequences for which at least one contig was recovered ranged from 31.9% (for *Lumbricus terrestris*,  
134 the species with the maximal divergence from the species used to design the baits) to 88.2% across  
135 species (median=78.8%, **Table 1**).

<b>Species</b>	<b>Group</b>	<b>Targeted transcripts</b>	<b>Recovered transcripts</b>	<b>Percentage of recovered among targeted transcripts</b>
<i>Formica fusca</i>	ants	1810	1427	78.8
<i>Formica sanguinea</i>	ants	1810	1396	77.1
<i>Formica pratensis</i>	ants	1810	1398	77.2
<i>Formica cunicularia</i>	ants	1810	1406	77.7
<i>Maniola jurtina</i>	butterflies	2235	1921	86.0
<i>Melanargia galathea</i>	butterflies	2235	1713	76.6
<i>Pyronia tithonus</i>	butterflies	2235	1823	81.6
<i>Pyronia bathseba</i>	butterflies	2235	1864	83.4
<i>Aphantopus hyperanthus</i>	butterflies	2235	1772	79.3
<i>Allolobophora chlorotica L1</i>	earth worms	2955	2293	77.6
<i>Allolobophora chlorotica L2</i>	earth worms	2955	2315	78.3
<i>Allolobophora chlorotica L4</i>	earth worms	2955	1732	58.6
<i>Aporrectodea icterica</i>	earth worms	2955	2321	78.5
<i>Lumbricus terrestris</i>	earth worms	2955	943	31.9
<i>Lineus sanguineus</i>	ribbon worms	1725	1251	72.5
<i>Lineus ruber</i>	ribbon worms	1725	1521	88.2
<i>Lineus lacteus</i>	ribbon worms	1725	1516	87.9
<i>Lineus longissimus</i>	ribbon worms	1725	1505	87.2
<i>Mytilus galloprovincialis</i>	mussels	2181	1820	83.4
<i>Mytilus edulis</i>	mussels	2181	1721	78.9
<i>Mytilus trossulus</i>	mussels	2181	1740	79.8
<i>Mytilus californianus</i>	mussels	2181	1808	82.9

136 **Table 1: Summary of the number of targeted transcripts recovered in the capture experiment.**

137 We assessed contamination between samples from distinct species using CroCo (33). Overall, the  
 138 inter-groups connection in **Figure S1** indicates a low level of cross-contamination: when there were  
 139 connections between taxonomic groups, on average they concerned 38 contigs identified as  
 140 contaminants, with the worst case being the 172 contigs identified as contaminants between the  
 141 assembly of *Lineus sanguineus* and *Mytilus galloprovincialis*. Connections between assemblies  
 142 from closely related species were very likely false positive cases, especially since the intensity of  
 143 the within-group connections was congruent with the phylogenetic distance between species within

144 taxa. Regardless, all contigs identified as potential contaminants were excluded from the dataset in  
145 downstream analyzes as a cautionary measure.

146 Within each group, we focused on orthologous contigs (**Table S2**), predicted open reading frames,  
147 and called the diploid genotypes of individuals for every coding position. The SNPs counts obtained  
148 after genotyping are summarized in **Table S3**. We obtain less than a thousand SNPs in only two  
149 species, the minimum being 153 for *Lineus longissimus*, in which we were only able to recover data  
150 for six individuals.

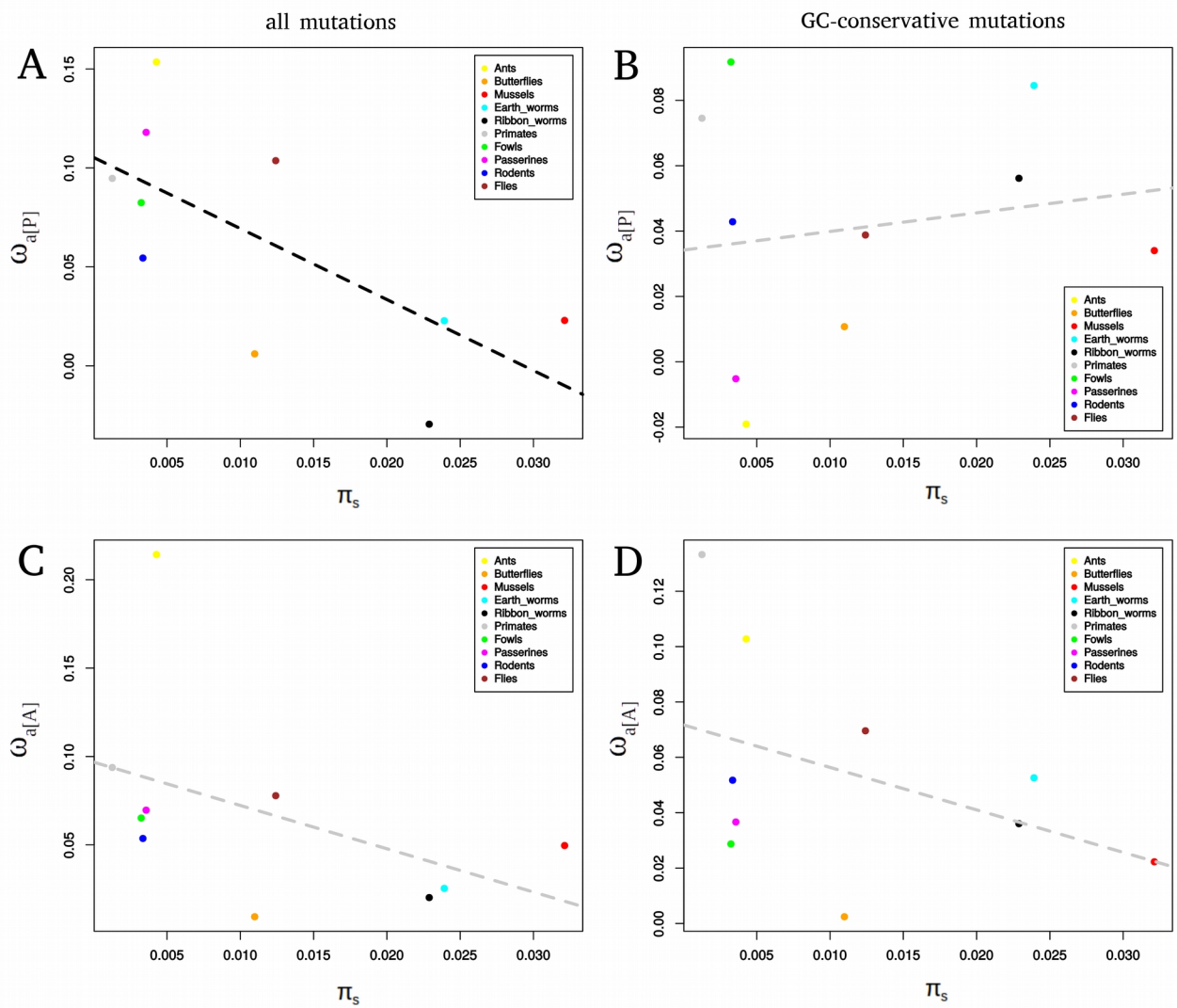
151 We recovered an average of 8,459 SNPs per species in ants, 7,950 in butterflies, 4,763 in earth  
152 worms, 8,347 in ribbon worms, 19,750 in mussels, 10,191 in primates, 25,534 in rodents, 40,870 in  
153 passerines, 8,488 in fowls and 195,398 in flies.

154 In conclusion, the capture experiment seems suitable for recovering population coding sequence  
155 data for several closely related species - here, the maximum divergence between species within a  
156 taxonomic group was 0.2 subst./site, i.e. the divergence between *Lumbricus terrestris* and  
157 *Allolobophora chlorotica* L1.

158 **2. Between-groups relationship between the population mutation rate ( $\theta$ ) and the adaptive  
159 substitution rate ( $\omega_a$ )**

160 We used Galtier's (2016) version of the MK method (18) introduced by Eyre-Walker and Keightley  
161 (2009) (16), accounting for the effect of slightly beneficial non-synonymous mutations (see  
162 **Methods**). Two strategies were adopted to combine SFS information from distinct species in a  
163 group-level estimate of  $\omega_a$ , thus accounting for the problem of phylogenetic non-independence  
164 between species. For both strategies, we first calculated the dN/dS ratio  $\omega$  at the group-level, i.e., by  
165 averaging across all branches of the tree (see Material and Methods). Our first estimator, which we  
166 called  $\omega_{a[P]}$ , was obtained by pooling SFS from distinct species within a group, separately for  
167 synonymous and non-synonymous SNPs (as in (34)), before fitting the model and estimating the  
168 parameters. This estimate combines data across species weighting each species equally, thus  
169 alleviating the effect of species-specific demographic history.

170 We then computed the relationship between  $\omega_{a[P]}$  estimates and the across-species average nucleotide  
171 diversity,  $\pi_s$ , which was taken as an estimate of  $\theta$ . We detected a significant negative relationship  
172 between  $\omega_{a[P]}$  and the across-species average nucleotide diversity,  $\pi_s$ , taken as an estimate of  $\theta$   
173 (regression test,  $r^2=0.4$ , p-value=2.9e-02) (**Figure 1A**).



174 **Figure 1: Relationship between group-level  $\omega_a$  and group-level  $\pi_s$ .**

175 A:  $\omega_a$  was estimated by pooling SFS across species within a group ( $\omega_{a[P]}$ ) using all mutations.

176 B:  $\omega_a$  was estimated by pooling SFS across species within a group ( $\omega_{a[P]}$ ) using only GC-conservative mutations.

177 C:  $\omega_a$  was estimated via the averaging of  $\omega_{na}$  across species within a group ( $\omega_{a[A]}$ ) using all mutations.

178 D:  $\omega_a$  was estimated via the averaging of  $\omega_{na}$  across species within a group ( $\omega_{a[A]}$ ) using only GC-conservative  
179 mutations.

180 Group level  $\pi_s$  was estimated by averaging species-level  $\pi_s$  across closely related species. Black dotted lines represent  
181 significant regressions across taxonomic groups and grey dotted lines non-significant ones.

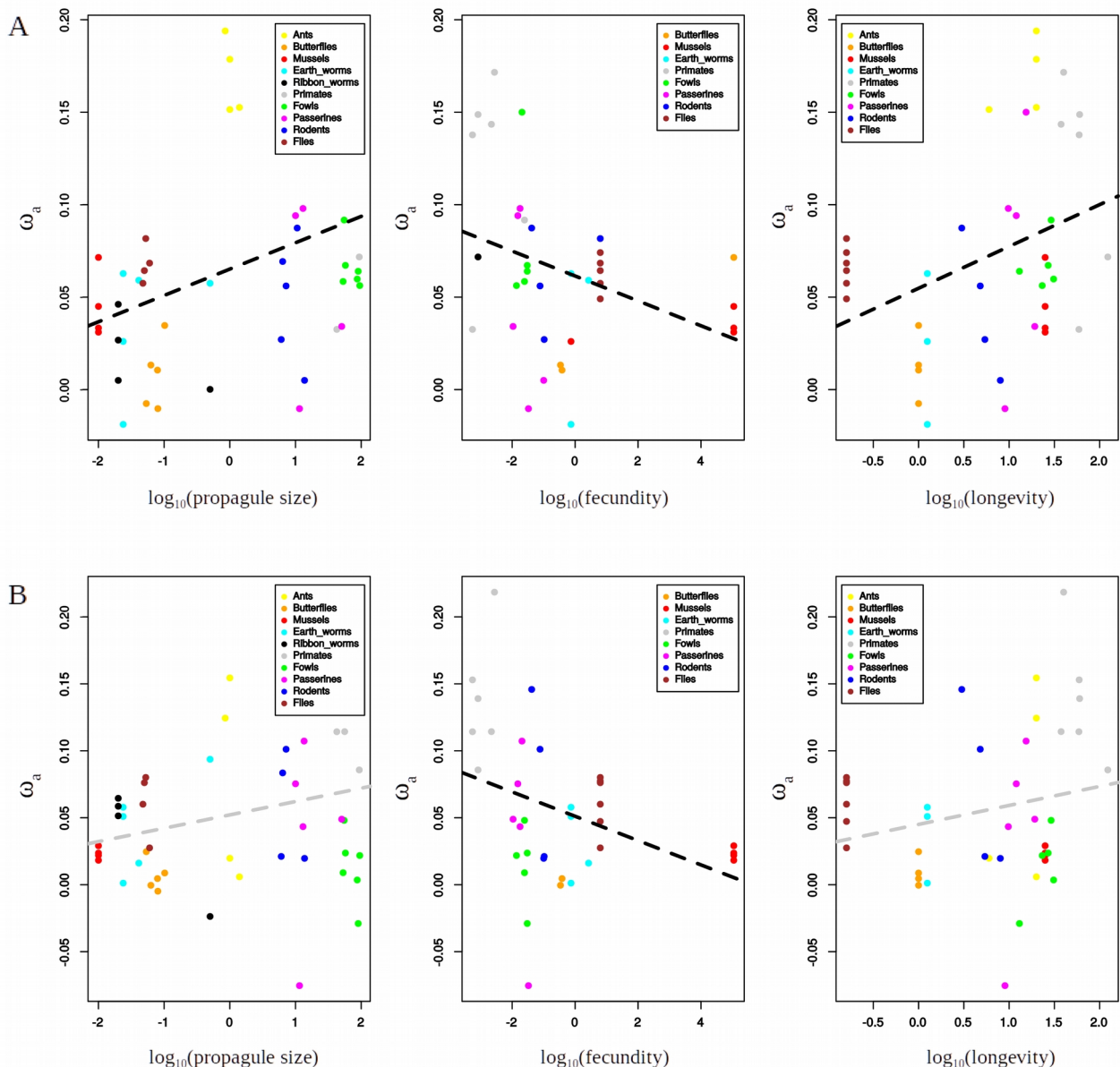
182 Recent studies in birds and more recently primates indicated that GC-biased gene conversion  
183 (gBGC) may lead to overestimation (25,26) or underestimation of  $\omega_a$  (27). Interestingly, gBGC does  
184 not affect genomic evolution with the same intensity in all organisms (35). To avoid bias in the  
185 estimation in species where gBGC is active, we restricted the SNP and substitution data to GC-

186 conservative changes, which are not influenced by gBGC. We found a non-significant positive  
187 correlation  $\omega_{a[P]GC\text{-conservative}}$  and  $\theta$  (**Figure 1B**).

188 Our second estimator of the adaptive rate at the group level, which we called  $\omega_{a[A]}$ , was obtained by  
189 calculating the across-species arithmetic mean of  $\omega_{na}$  within a group, and by then subtracting this  
190 average from  $\omega$ . We suggest that  $\omega_{a[A]}$  is a reasonable estimator of the adaptive rate with fluctuating  
191 population size if the pace of fluctuations is sufficiently slow, such that the sampled species have  
192 reached the selection/drift equilibrium (Supplementary Material **Box S1**). We found a non-  
193 significant negative correlation between  $\omega_{a[A]}$  and  $\omega_{a[A]GC\text{-conservative}}$  and  $\pi_s$  (**Figure 1C and 1D**). Overall,  
194 the between-group analysis seems to confirm the absence of a positive relationship between  $\omega_a$  and  
195  $\theta$  at the between-phyla scale in animals, and even suggests the existence of a weak, negative  
196 relationship.

197 **3. Relationship between life history traits and  $\omega_a$**

198 We used several life history traits known to be correlated with species long-term effective  
199 population size (36). In our data set, all life history traits were correlated with  $\pi_s$  (Spearman  
200 correlation p-value, propagule size: 1.1e-12, adult size: 4.3e-04, longevity: 5.5e-02, body mass:  
201 4.7e-03, fecundity: 9.4e-06). When estimating the per-group  $\omega_a$ , we did not find any significant  
202 relationship with life history traits, but the signs of the correlation coefficients were indicative of a  
203 negative relationship between the long-term  $N_e$  and both  $\omega_a$  and  $\omega_{a[GC\text{-conservative}]}$  (**Figures S2 and S3**).  
204 When considering all 50 species (i.e. without controlling for phylogenetic inertia) and all mutations,  
205 we found a negative relationship between  $\omega_a$  and  $\log_{10}$  transformed fecundity (regression test,  
206  $r^2=0.094$ ), as well as a positive relationship with  $\log_{10}$  transformed longevity (regression test,  
207  $r^2=0.10$ ) and  $\log_{10}$  transformed propagule size (regression test,  $r^2=0.13$ ) (**Figure 2A**). When using  
208 only GC-conservative mutations, the relationships were similar (regression test,  $r^2=0.11$ ) (**Figure**  
209 **2B**).



210 **Figure 2: Relationship between species-level  $\omega_a$  and life history traits.**

211 A:  $\omega_a$  is estimated using all mutations.

212 B:  $\omega_a$  is estimated using only GC-conservative mutations.

213 Black dotted lines represent significant regressions across taxonomic groups and grey dotted lines non-significant ones.

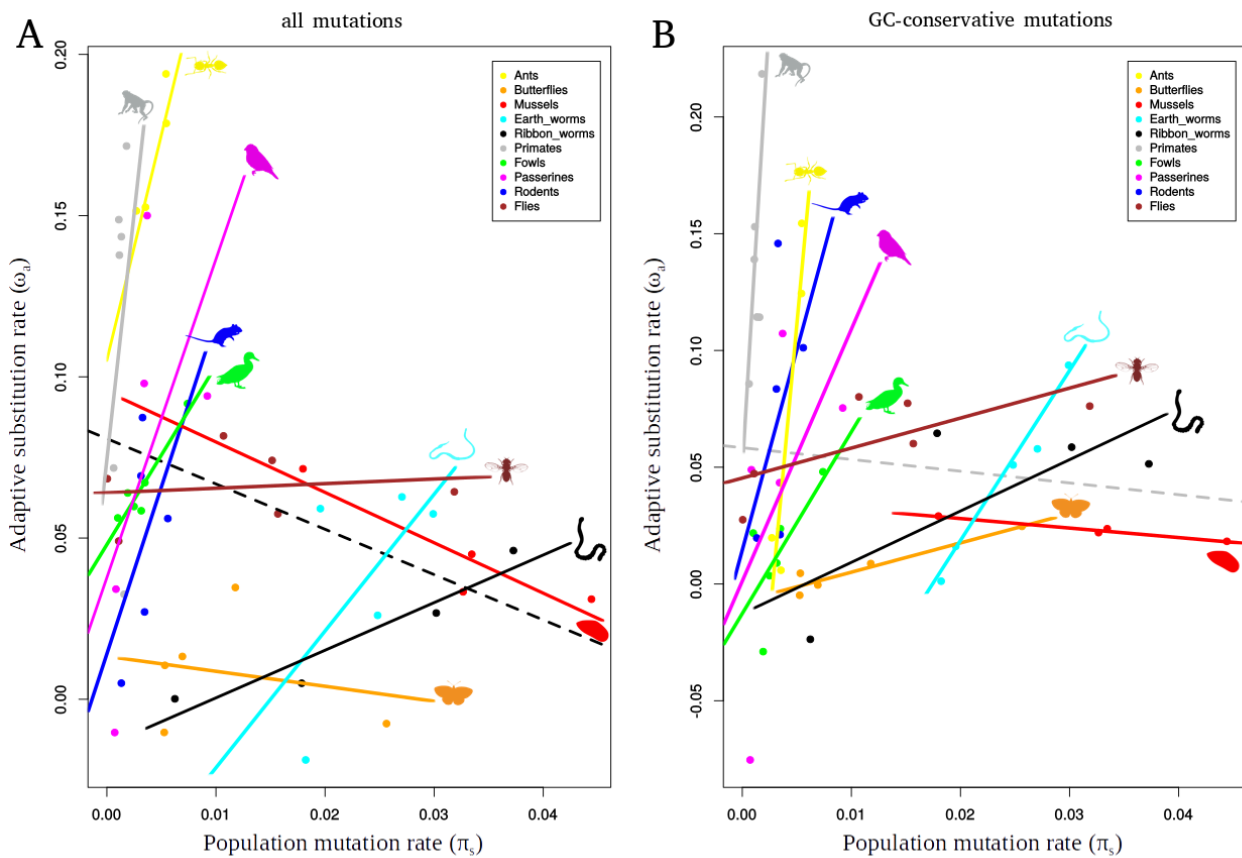
214 We also found a **negative** relationship between  $\omega_{na}$  and fecundity (regression test  $r^2=0.31$ ), and a  
 215 **positive** relationship between  $\omega_{na}$  and propagule size (regression test  $r^2=0.13$ ) and body mass  
 216 (regression test  $r^2=0.10$ ), which was also true when using only GC-conservative mutations: **positive**  
 217 relationships between  $\omega_{na[GC\text{-conservative}]}$  and propagule size (regression test  $r^2=0.21$ ), longevity

218 (regression test  $r^2=0.12$ ), body mass (regression test  $r^2=0.08$ ) and a negative relationship with  
219 fecundity (regression test  $r^2=0.36$ ) (**Figure S4**).

220 **4. Within-group relationship between  $\theta$  and  $\omega_a$**

221 To assess the within-group effect of  $\pi_s$  on  $\omega_a$ , we performed an analysis of covariance (ANCOVA)  
222 with the taxonomic group as a categorical independent variable, as in (29). The principle of this  
223 analysis is to fit a set of parallel lines (one for each taxonomic group) and test whether their  
224 common slope is significantly different from zero. Moreover, we tested if the relationship between  
225  $\omega_a$  and  $\pi_s$  or life history traits differs between taxonomic groups by testing whether the lines have  
226 different intercepts.

227 By this strategy, we found that  $\omega_a$  and both  $\pi_s$  and  $\log_{10}(\pi_s)$  were significantly positively correlated  
228 when using only GC-conservative mutations (ANCOVA p-value=2.8e-02 and 3.1e-03, respectively)  
229 (**Figure 3B**).  $\omega_a$  was only marginally positively correlated with  $\log_{10}(\pi_s)$  when using all mutations  
230 (ANCOVA p-value=7.6e-02) (**Figure 3A**). We also found that there was a significant variation  
231 between the intercepts (ANCOVA p-value<1e-03), as well as a significant interaction between the  
232 dependent variable and the categorical independent variable (ANOVA p-value=1.6e-02). Those  
233 results support the existence of a positive relationship between  $\omega_a$  and  $\theta$  within groups, with the  
234 slope of the relationship differing between groups. This is consistent with the hypothesis that within  
235 a group, higher- $\theta$  species are more likely to find and fix adaptive substitutions than low- $\theta$  species, in  
236 line with the hypothesis that mutation limits adaptation. **Figure 3** shows that the slopes of the  
237 within-group  $\omega_a/\theta$  correlations decreased with group-level  $\pi_s$ , and we actually found a significant  
238 negative correlation between these two quantities both when using all or only GC-conservative  
239 mutations (Spearman correlation coefficient=-0.77, p-value=1.4e-02). This interestingly suggests  
240 that the limitation of adaptation by the supply of adaptive mutations is effective and strong in small-  
241  $\theta$  groups (e.g. primates, rodents, ants), but not in high- $\theta$  groups of animals (e.g. flies, mussels,  
242 butterflies), where the  $\omega_a/\theta$  relationship is essentially flat (**Figure 3**).



243 **Figure 3: Relationship between species-level  $\omega_a$  and  $\pi_s$ .**

244 A:  $\omega_a$  is estimated using all mutations.

245 B:  $\omega_a$  is estimated using only GC-conservative mutations.

246 Black dotted lines represent significant regressions across taxonomic groups and grey dotted lines non-significant ones.

247 When analyzing the per-species non-adaptive substitution rate, we found a global negative  
 248 relationship between  $\omega_{na}$  and  $\pi_s$  (using both all mutations and only GC-conservative mutations:  
 249 regression test  $r^2=0.16$  and  $r^2=0.33$ , respectively), and a significantly negative relationship within  
 250 groups (ANCOVA  $p\text{-value}=1.9e-02$  and  $p\text{-value}=1.8e-03$ , respectively) (**Figure S4**). This was  
 251 consistent with the expectations of the nearly neutral theory of evolution (28), and with previous  
 252 empirical results (18,37). The estimated ratio of adaptive to total non-synonymous substitutions,  $\alpha$ ,  
 253 behaved more or less similarly to  $\omega_a$  (**Figure S5**).

254 **5. Control for fluctuations in  $N_e$** 

255 We were concerned that the **positive** correlation between  $\omega_a$  and  $\pi_s$  might have been due to an  
256 artifact generated by past fluctuations in population size (23,24). To test this, we simulated coding  
257 sequence evolution under several demographic scenarios with four regimes of demographic  
258 fluctuations, with a three or thirty-fold ratio between the low and high  $N_e$ , and a high or low long-  
259 term  $N_e$  (see Material and Method and **Figure S6**). We found that the only scenario where  
260 demographic fluctuations could lead to a detectable positive correlation between  $\omega_a$  and  $\pi_s$  was that  
261 with the highest long-term  $N_e$  and highest difference between the low and high  $N_e$  (see **Figure S7**  
262 **panel B**, regression test  $r^2=0.07$ ,  $p\text{-value}=9.5\text{e-}03$ ). The correlation disappeared when we used a  
263 ten-fold smaller long-term  $N_e$ , whereas we empirically observed that the correlation between  $\omega_a$  and  
264  $\pi_s$  was stronger for small long-term  $N_e$  groups (**Figure 2**). These simulations therefore suggested  
265 that ancient demographic fluctuations could not explain our finding of a positive within-group  
266 correlation between  $\omega_a$  and  $\pi_s$  in low- $\theta$  groups. **We also checked that the  $F_{is}$  statistics was not**  
267 **significantly correlated to  $\omega_a$  (regression test  $p\text{-value}=5.9\text{e-}01$ ) or  $\pi_s$  ( $p\text{-value}=2.9\text{e-}01$ ), which**  
268 **indicated that population substructure was unlikely to confound our results.**

269 **DISCUSSION**270 **1. Influence of  $\theta$  on  $\omega_a$  : a two-scale mechanism**

271 In this study, we analyzed a 50-species population genomic data set to assess the relationship  
272 between the adaptive substitution rate and the population mutation rate and test the hypothesis that  
273 mutation limits adaptation in natural populations of animals.

274 We found that the relationship between  $\omega_a$  and  $\theta$  depended on the considered timescale, **which is**  
275 **expected if the assumption of a fixed DFE across divergent taxa does not hold.** At a recent  
276 evolutionary scale (i.e., neutral divergence  $<0.2$  subst./site), we found a significant positive  
277 correlation between  $\omega_a$  and  $\pi_s$  (**Figure 2**). Interestingly, the slope of the relationship differed  
278 significantly among taxonomic groups, and this slope itself was negatively correlated with the  
279 group average  $\pi_s$ . Otherwise, estimates at the group level revealed a weak but consistently negative  
280 relationship between  $\omega_a$  and  $\pi_s$ , and between  $\omega_a$  and various life history traits correlated with the  
281 long-term  $N_e$  (**Figure 1 and 3**). This time scale-dependent behavior of the  $\omega_a/\theta$  relationship was here

282 demonstrated via the analysis of a single, multi-scale dataset, somehow reconciling earlier taxon-  
283 specific studies on the subject (4,8,18,29–31,38).

284 **2. Relationship between  $\theta$  and  $\omega_a$  - a real causative link or an artifact ?**

285 Our ANCOVA analysis revealed that the slopes of the relationships between  $\omega_a$  and  $\pi_s$  within each  
286 taxonomic group were significantly different from zero, demonstrating the existence of a positive  
287 link between  $\omega_a$  and  $\pi_s$  within groups (**Figure 2**). We were concerned that this relationship may have  
288 resulted from a bias in the MK approach, instead of being a true biological signal. Indeed, the MK  
289 approach implicitly assumes that the regime of selection/drift has been constant over the considered  
290 time period, i.e. since the divergence between the focal and outgroup species. If however the  
291 selection/drift regime had changed (e.g. via a change in effective population size) between the  
292 period during which divergence had accumulated and the period during which polymorphism was  
293 built, this could lead to overestimation or underestimation of  $\omega_a$  (23,24). Here, we used the so-called  
294  $r_i$ 's nuisance parameters (39) to control for recent changes in  $N_e$ .

295 In contrast, ancient  $N_e$  changes that affect coding sequence divergence are virtually impossible to  
296 trace. We showed in a previous simulation-based study that ancient demographic fluctuations could  
297 lead to severely overestimated  $\alpha$  and  $\omega_a$  - an upward bias which is exacerbated when the true  
298 adaptive substitution rate is low (23). Moreover, it has been shown by modeling single changes in  
299  $N_e$  that in the presence of slightly deleterious mutations, an increase in  $N_e$  in the past could yield  
300 spurious evidence of positive selection, which can lead to a spurious positive correlation between  $\omega_a$   
301 and  $\pi_s$  (24).

302 We used simulations to test if demographic fluctuations could lead to such a correlation. Our results  
303 suggested that long-term fluctuations were not responsible for the positive link between  $\omega_a$  and  $\pi_s$   
304 that we report. In addition, the gradual decrease in the slope of the relationship with per-group  
305 average  $\pi_s$  was also consistent with the fact that the relation is genuine, because (i) we do not expect  
306 the demographic fluctuation regime to correlate with the average  $\pi_s$  of the group, and (ii) there was  
307 no relationship between the inter-group variation in  $\pi_s$  and the average  $\pi_s$  of the group (Spearman  
308 correlation test: p-value=4.7e-01).

309 A recently developed method allows the estimation of  $\alpha$  and  $\omega_a$  using polymorphism data alone  
310 (20), thus avoiding the assumption of time constancy of the drift/selection regime. However,

311 estimates of  $\alpha$  and  $\omega_a$  by this method deserve a specific interpretation, as they represent the rate of  
312 adaptive evolution of the species during its very recent history, and not the one of its long-term  
313 history. This method requires high quality datasets and highly polymorphic species, and it was not  
314 applicable to our dataset, in which species and groups differ widely in terms of SNP numbers  
315 (**Table S3**).

316 **3. Mutation limits adaptation within taxonomic groups in small- $\theta$  animals**

317 Our findings therefore indicate of a genuine link between the adaptive substitution rate and  $\theta$ , which  
318 is consistent with the hypothesis that, in several groups of animals, the rate of adaptation is limited  
319 by the supply of beneficial mutations. The slope of the relationship was particularly steep in ants,  
320 fowls, passerines, rodents and primates (**Figure 2**). For instance, the estimated adaptive rate in  
321 rhesus macaque (*Macaca mulatta*:  $\pi_s=0.0018$ ) was more than 3-fold higher than that of humans  
322 (*Homo sapiens*:  $\pi_s=0.0006$ ). Note that this interpretation relies on the assumption that different  
323 species from a given taxonomic group share the same DFE and, in particular, the same proportion  
324 of beneficial mutations. This is consistent with previous analyses of the relationship between  $\omega_a$  and  
325  $\pi_s$  at a relatively recent time scale (27,29). It is also consistent with the finding that strong selective  
326 sweeps are more abundant in species of great apes with a large population size (4).

327 Interestingly, we found that the relationship between  $\omega_a$  and  $\pi_s$  was significantly stronger in low-  
328 diversity than high-diversity groups. In flies, a high-diversity group, the slope of the linear  
329 regression between the two variables was only 1.3, whereas it was between 7.8 and 77 in the four  
330 vertebrate groups. In mussels, i.e. the taxonomic group with the highest average diversity in our  
331 dataset, we detected no significant relationship between  $\omega_a$  and  $\pi_s$ , with the slope being very close to  
332 zero (-0.4). It is possible that in such organisms the adaptive evolutionary rate is not limited by the  
333 mutation supply: the standing variation and/or the influx of new mutations are sufficient for proteins  
334 to find the required alleles. This is consistent with the results of (8), who showed that patterns of  
335 adaptation to insecticides in natural *Drosophila melanogaster* populations are incompatible with the  
336 hypothesis that adaptation is mutation-limited. This is also consistent with the results of Jensen and  
337 Bachtrog (40), who found very similar rates of adaptation between two *Drosophila* species with  
338 different  $N_e$ .

Finally, the results shown in **Figure 3** corroborate theoretical predictions indicating that when  $N_e$  is sufficiently large, it is the species ability to combine beneficial alleles across loci that limits adaption rather than the strength of selection or the mutation supply (9). Our results suggest that this situation applies to large- $N_e$  groups of animals, such as *Drosophila*, but not to small- $N_e$  ones, such as primates. Indeed, one should keep in mind that the two variables we analyze here,  $\pi_s$  and  $\omega_a$ , are potentially affected by the effects of interference between segregating mutations (17). Weissman & Barton (9), following Gillespie (41), explicitly modeled linkage between beneficial mutations and showed that the effect of  $N_e$  on the adaptive rate is expected to saturate when parameters are set to values estimated in *Drosophila*. The neutral genetic diversity is also expected to be affected by linked selection (42,43), to an extent that still deserves to be properly assessed (44)]. Quantifying the effect of linked selection on the neutral and selected variation, and its relationship with  $N_e$ , is a current challenge and would help interpreting results such as the ones we report here.

#### 4. What are the determinants of $\omega_a$ across distantly related taxa?

We used two approaches to estimate the adaptive substitution rate at the group level. Both supported a negative among-group relationship between  $\omega_a$  and  $\pi_s$ , and between  $\omega_a$  and life history traits that have been shown to be linked to the long-term effective population size (36) (**Figure 1, S2, S3** and 3). As different sets of genes were used in the different groups of animals, the gene content might have influenced our results. Indeed, Enard et al. (45) showed that genes interacting with viruses experience a significantly higher adaptive substitution rate, thus demonstrating the importance of the gene sampling strategy in comparative studies. In the exon capture experiment, a subset of genes were randomly sampled from an existing transcriptome reference, whereas all available genes were used in the other species (provided that they were present in all species within a group). We do not see any particular reason why the gene sample would be biased with respect to virus interacting proteins in some specific groups, and we did not detect any effect of data type (i.e. exon capture vs. genome-wide) on  $\omega_a$ . Our results are consistent with the results of Galtier (16), who analyzed the relationship between  $\omega_a$  and  $\pi_s$  in a transcriptomic dataset of 44 distantly related species of animals. Indeed, the main analysis in Galtier (18) revealed no significant correlation between  $\omega_a$  and  $\pi_s$ , but various control analyses (particularly using GC or expression restricted datasets) yielded a significantly negative correlation between the two variables.

368 This suggests that the mutation limitation hypothesis does not accurately account for the variation  
369 of  $\omega_a$  at a large taxonomic scale, implying that factors other than  $\theta$  must be at work here. Hereafter  
370 we discuss a number of such potential factors in the light of Fisher's geometrical model (FGM),  
371 which provides a convenient framework for considering the determinants of the adaptive  
372 substitution rate.

373 First, simulations under FGM and a moving optimum showed that the adaptive substitution rate is  
374 primarily determined by the rate of environmental change (32,46). If one assumes that species with  
375 a longer generation time undergo a higher per generation rate of environmental change, and that  
376 generation time is negatively correlated to population size in animals, then our results could perhaps  
377 be interpreted this way (36).

378 Moreover, Lourenço et al. (32) suggested that organismal complexity, represented by the  
379 dimensionality of the phenotypic space in FGM, affects the adaptive substitution rate more strongly  
380 than the effective population size does, with the adaptive substitution rate being an increasing  
381 function of complexity. This is because the probability that a new mutation is in the optimal  
382 direction decreases as the number of potential directions increases, such that the average adaptive  
383 walk takes more steps in a high-dimension than a low-dimension space (32,47). Complexity *sensus*  
384 FGM, however, is very hard to quantify in a biologically relevant way. To argue that primates and  
385 birds are more complex than mussels and worms does not seem particularly relevant when  
386 considering the organism level. Different measures of complexity have been considered at the  
387 molecular or cellular level, such as genome size, gene or protein number, number of protein-protein  
388 interactions, number of cell types, and these seem to point towards a higher complexity in mammals  
389 than insects, for instance (37,38). This is consistent with the idea of a greater complexity of species  
390 with smaller  $N_e$ . Fernández and Lynch (50) suggested that the accumulation of mildly deleterious  
391 mutations in small  $N_e$  populations induces secondary selection for protein-protein interactions that  
392 stabilize key gene functions, thus introducing a plausible mechanism for the emergence of  
393 molecular complexity (50). If the number of protein-protein interactions is a relevant measure of  
394 proteome complexity, then this might contribute to explain our findings of a higher adaptive  
395 substitution rate in low- $\theta$  than in high- $\theta$  groups.

396 Finally, variations in  $\omega_a$  across distantly related taxa could be modulated by the long-term  $N_e$  via  
397 the mean distance of the population to the fitness optimum. Indeed, under FGM, the proportion of  
398 beneficial mutations increases with the distance to the optimum. Groups of species evolving under  
399 small long-term  $N_e$  are further away from their optimum, compared to larger- $N_e$  groups, due to an

400 increased rate of fixation of deleterious mutations at equilibrium, so they are predicted to undergo a  
401 larger proportion of beneficial, compensatory mutations. Empirical analyses of SFS based on large  
402 samples in humans and flies are consistent with the hypothesis that humans are on average more  
403 distant to their optimum than flies (11).

404 To sum up, our results suggest that factors linked to species long-term effective population size  
405 affect the DFE, i.e., the proportion and rate of beneficial mutation would be non-independent of the  
406 long-term  $N_e$ . We suggest that the proteome is probably more complex and further away from its  
407 optimal state in small- $N_e$  than in large- $N_e$  groups of animals, which might contribute to increasing  
408 the steady-state adaptive rate in the former, thus masking the effect of mutation limitation in across-  
409 group comparisons.

## 410 CONCLUSION

411 In this study, we sampled a large variety of animals species and demonstrated a timescale-dependent  
412 relationship between the adaptive substitution rate and the population mutation rate, that reconciles  
413 previous studies that were conducted at different taxonomic scales. We demonstrate that the  
414 relationship between the adaptive substitution rate and  $\theta$  within closely related species sharing a  
415 similar DFE is shaped by the limited beneficial mutation supply, whereas the between-group pattern  
416 probably reflects the influence of long-term population size on the proportion of beneficial  
417 mutations. Our results provide empirical evidence for mutation-limited adaptive rate at whole  
418 proteome level in small- $N_e$  groups of animals, while stressing the fact that DFE is not independent  
419 of the long-term effective population size – a crucial factor that must be properly accounted for in  
420 large-scale comparative population genomic analyses.

## 421 MATERIAL & METHODS

### 422 1. Data set

423 Genomic, exomic and transcriptomic data from primates, passerines, fowls, rodents and flies were  
424 retrieved from the SRA database. Detailed referenced, bioprojects and sample sizes are provided in

425 **Table S1.** The minimal sample size was five diploid individuals (in *Papio anubis*) and the  
426 maximum was 20 (in seven species).

427 Exon capture data were newly generated in ants, butterflies, mussels, earth worms and ribbon  
428 worms. We gathered tissue samples or DNA samples for at least eight individuals per species and  
429 four or five species per group. Reference transcriptomes were obtained from previously published  
430 RNA-seq data in one species per taxonomic group (36,51,52). Details of the species and numbers of  
431 individuals are presented in **Table S1**.

432 **2. Multiplexed target capture experiment**

433 DNA from whole animal body (ants), body section (earth worms, ribbon worms), mantle (mussels)  
434 or head/thorax (butterflies) was extracted using DNAeasy Blood and Tissue kit (QIAGEN)  
435 following the manufacturer instructions. About 3 µg of total genomic DNA were sheared for 20 mn  
436 using an ultrasonic cleaning unit (Elmasonic One). Illumina libraries were constructed for all  
437 samples following the standard protocol involving blunt-end repair, adapter ligation, and adapter  
438 fill-in steps as developed by (53) and adapted in (54).

439 To perform target capture, we randomly chose contigs in five published reference transcriptomes  
440 (*Maniola jurtina* for butterflies (51), *Lineus longissimus* for ribbon worms (36), *Mytilus*  
441 *galloprovincialis* for mussels (36), *Allobophora chlorotica L1* for earth worms (36), and *Formica*  
442 *cunicularia* for ants (52)) in order to reach 2Mb of total sequence length per taxon (~2000 contigs).  
443 100nt-long baits corresponding to these sequences were synthesized by MYbaits (Ann Arbor, MI,  
444 USA), with an average cover of 3X.

445 We then performed multiplexed target capture following the MYbaits targeted enrichment protocol:  
446 about 5 ng of each library were PCR-dual-indexed using Taq Phusion (Phusion High-Fidelity DNA  
447 Polymerase Thermo Scientific) or KAPA HiFi (2× KAPA HiFi HotStart ReadyMix  
448 KAPABIOSYSTEMS) polymerases. We used primers developed in (55). Indexed libraries were  
449 purified using AMPure (Agencourt) with a ratio of 1.6, quantified with Nanodrop ND-800, and  
450 pooled in equimolar ratio. We had a total of 96 combinations of indexes, and two Illumina lanes, for  
451 a total of 244 individuals. This means that we had to index two (rarely three) individuals with the  
452 same combination to be sequenced in the same line. When this was necessary, we assigned the same  
453 tag to individuals from distantly related species (i.e. from different groups). Exon capture was  
454 achieved according to the Mybaits targeted enrichment protocol, adjusting the hybridization

455 temperature to the phylogenetic distance between the processed library and the baits. For libraries  
456 corresponding to individuals from the species used to design baits, we used a temperature of 65°C  
457 during 22 h. For the other ones we ran the hybridization reactions for 16 h at 65°C, 2 h at 63°C, 2 h  
458 at 61°C and 2 h at 59°C. Following hybridization, the reactions were cleaned according to the kit  
459 protocol with 200 µL of wash buffers, and hot washes were performed at 65°C or 59°C depending  
460 on the samples. The enriched solutions were then PCR-amplified for 14 to 16 cycles, after removal  
461 of the streptavidin beads. PCR products were purified using AMPure (Agencourt) with a ratio of  
462 1.6, and paired-end sequenced on two Illumina HiSeq® 2500 lines. Illumina sequencing and  
463 demultiplexing were subcontracted.

464 **3. Assembly and genotyping**

465 For RNA-seq data (i.e. fowls and two rodents), we used trimmomatic (56) to remove Illumina  
466 adapters and reads with a quality score below 30. We constructed *de novo* transcriptome assemblies  
467 for each species following strategy B in (57), using Abyss (58) and Cap3 (59). Open reading frames  
468 (ORFs) were predicted using the Trinity package (60). Contigs carrying ORF shorter than 150 bp  
469 were discarded. Filtered RNA-seq reads were mapped to this assembly using Burrow Wheeler  
470 Aligner (BWA) (version 0.7.12-r1039) (61). Contigs with a coverage across all individual below  
471 2.5xn (where n is the number of individuals) were discarded. Diploid genotypes were called  
472 according to the method described in (62) and (63) (model M1) via the software reads2snps  
473 (<https://kimura.univ-montp2.fr/PopPhyl/index.php?section=tools>). This method calculates the  
474 posterior probability of each possible genotype in a maximum likelihood framework. Genotypes  
475 supported by a posterior probability higher than 95% are retained, otherwise missing data is called.  
476 We used version of the method which accounts for between-individual, within-species  
477 contamination as introduced in (52), using the -contam=0.1 option, which means assuming that up  
478 to 10% of the reads assigned to one specific sample may actually come from a distinct sample, and  
479 only validating genotypes robust to this source of uncertainty.

480 For primates, rodents, passerines and flies, reference genomes, assemblies and annotations files  
481 were downloaded from Ensembl (release 89) and NCBI (**Table S1**). We kept only 'CDS' reports in  
482 the annotations files, corresponding to coding exons, which were annotated with the automatic  
483 Ensembl annotation pipeline, and the havana team for *Homo sapiens*. We used trimmomatic to  
484 remove Illumina adapters, to trim low-quality reads (i.e. with an average base quality below 20),

485 and to keep only reads longer than 50bp. Reads were mapped using BWA (61) on the complete  
486 reference assembly. We filtered out hits with mapping quality below 20 and removed duplicates,  
487 and we extracted mapping hits corresponding to regions containing coding sequences according to  
488 the annotated reference assembly. This was done to avoid calling SNPs on the whole genome,  
489 which would be both time consuming and useless in the present context. We called SNPs using a  
490 pipeline based on GATK (v3.8-0-ge9d80683). Roughly, this pipeline comprised two rounds of  
491 variant calling separated by a base quality score recalibration. Variant calling was first run on every  
492 individuals from every species using HaplotypeCaller (--emitRefConfidence GVCF  
493 --genotyping\_mode DISCOVERY -hets 0.001). The variant callings from all individuals of a given  
494 species were then used to produce a joint genotype using GenotypeGVCFs. Indels in the resulting  
495 vcf files were then filtered out using vcftools. The distributions of various parameters associated  
496 with SNPs were then used to set several hard thresholds (i.e. Quality by Depth < 3.0; Fisher Strand  
497 > 10; Strand Odds Ratio > 3.0; MQRootMeanSquare < 50; MQRankSum < -0.5; ReadPosRankSum  
498 < -2.0) in order to detect putative SNP-calling errors using VariantFiltration. This erroneous SNPs  
499 were then used for base quality score recalibration of the previously created mapping files using  
500 BaseRecalibrator. These mappings with re-calibrated quality scores were then used to re-call  
501 variants (HaplotypeCaller), to re-produce a joint genotype (GenotypeGVCFs, --allsites) and to re-  
502 set empirical hard thresholds (i.e. same values as above, except for Quality by Depth < 5.0). The  
503 obtained vcf files were converted to fasta files (i.e. producing two unphased allelic sequences per  
504 individual) using custom python scripts while discarding exons found on both mitochondrial and  
505 sexual chromosomes and while filtering out additional SNPs: we removed SNPs with a too high  
506 coverage (thresholds were empirically set for each species), with a too low coverage (i.e. 10x per  
507 individual) and with a too low genotype quality per individual (i.e. less than 30).

508 For reads generated through target capture experiment, we cleaned reads with trimomatic to  
509 remove Illumina adapters and reads with a quality score below 30. For each species, we chose the  
510 individual with the highest coverage and constructed de novo assemblies using the same strategy as  
511 in fowls. Reads of each individuals were then mapped to the newly generated assemblies for each  
512 species, using BWA (61). Diploid genotypes were called using the same protocol as in fowls. We  
513 used a version of the SNP calling method which accounts for between-individual, within-species  
514 contamination as introduced in (52) (see the following section). As the newly generated assemblies  
515 likely contained intronic sequences, the predicted cDNAs were compared to the reference  
516 transcriptome using blastn searches, with a threshold of e-value of 10e-15. We used an in-house

517 script to remove any incongruent correspondence or inconsistent overlap between sequences from  
518 the transcriptomic references and the predicted assemblies, and removed six base pairs at each  
519 extremity of the resulting predicted exonic sequences. These high-confidence exonic sequences  
520 were used for downstream analyses.

521 **3. Contamination detection and removal**

522 For the newly generated data set, we performed two steps of contamination detection. First, we used  
523 the software tool CroCo to detect inter-specific contamination in the *de novo* assembly generated  
524 after exon capture (33).

525 CroCo is a database-independent tool designed to detect and remove cross-contaminations in  
526 assembled transcriptomes of distantly related species. This program classifies predicted cDNA in  
527 five categories, “clean”, “dubious”, “contamination”, “low coverage” and “high expression”.  
528 Secondly, we used a version of the SNP calling method which accounts for between-individual,  
529 within-species contamination as introduced in (52), using the -contam=0.1 option. This means  
530 assuming that up to 10% of the reads assigned to one specific sample may actually come from a  
531 distinct sample, and only validating genotypes robust to this source of uncertainty.

532 **4. Orthology prediction and divergence analysis**

533 In primates, we extracted one-to-one orthology groups across the six species from the OrthoMaM  
534 database (64,65).

535 In fowls, passerines, rodents and flies, we translated the obtained CDS into proteins and predicted  
536 orthology using OrthoFinder (66). In fowls, full coding sequences from the well-annotated chicken  
537 genome (Ensembl release 89) were added to the dataset prior to orthology prediction, then  
538 discarded. We kept only orthogroups that included all species. We aligned the orthologous  
539 sequences with MACSE (Multiple Alignment for Coding SEquences (67).

540 In each of earth worms, ribbon worms, mussels, butterflies and ants, orthogroups were created via a  
541 a blastn similarity search between predicted exonic sequences reference transcriptomes. In each  
542 taxon, we concatenated the predicted exonic sequences of each species that matched the same ORF  
543 from the reference transcriptome and aligned these using MACSE. We then kept alignments  
544 comprising exactly one sequence per species or if only one species was absent.

545 We estimated lineage specific dN/dS ratio using bppml (version 2.4) and MapNH (version 2.3.2)  
546 (68), the former for estimating each branch length and the latter for mapping substitutions on  
547 species specific branches.

548 Tree topologies were obtained from the literature (**Table S4**). In passerines, fowls, rodents, flies and  
549 primates, we kept only alignments comprising all the species. In the other groups we also kept  
550 alignments comprising all species but one.

551 We also estimated dN/dS ratios at group level by adding up substitution counts across branches of  
552 the trees, including internal branches.

553 To account for GC-biased gene conversion, we modified the MapNH software such that only GC-  
554 conservative substitutions were recorded (26). We estimated the non-synonymous and synonymous  
555 number of GC-conservative sites per coding sequence using an in-house script. We could then  
556 compute the dN/dS ratio only for GC-conservative substitutions.

## 557 **5. Polymorphism analysis**

558 For each taxon, we estimated ancestral sequences at each internal node of the tree with the Bio++  
559 program SeqAncestor (68). The ancestral sequences at each internal node were used to orientate  
560 single nucleotide polymorphisms (SNPs) of species that descend from this node. We computed non-  
561 synonymous ( $\pi_n$ ) and synonymous ( $\pi_s$ , i.e.  $\theta$ ) nucleotide diversity, as well as  $\pi_n/\pi_s$  using the software  
562 dNdSpiNpiS\_1.0 developed within the PopPhyl project ([https://kimura.univ-  
563 montp2.fr/PopPhyl/index.php?section=tools](https://kimura.univ-montp2.fr/PopPhyl/index.php?section=tools)) (using gapN\_site=4, gapN\_seq=0.1 and median  
564 transition/transversion ratio values estimated by bppml for each taxonomic group). We also  
565 computed unfolded and folded synonymous and non-synonymous site frequency spectra both using  
566 all mutations and only GC-conservative mutations using an in-house script as in (18).

## 567 **6. Mc-Donlad-Kreitman analysis**

568 We estimated  $\alpha$ ,  $\omega_a$  and  $\omega_{na}$  using the approach of (16) as implemented in (18) (program Grapes  
569 v.1.0). It models the distribution of the fitness effects (DFE) of deleterious and neutral non-  
570 synonymous mutations as a negative Gamma distribution, which is fitted to the synonymous and  
571 non-synonymous site frequency spectra (SFS) computed for a set of genes. This estimated DFE is  
572 then used to deduce the expected dN/dS under near-neutrality. The difference between observed and

573 expected dN/dS provides an estimate of the proportion of adaptive non-synonymous substitutions,  
574  $\alpha$ . The per mutation rate of adaptive and non-adaptive amino-acid substitution were then obtained as  
575 following:  $\omega_a = \alpha(dN/dS)$  and  $\omega_{na} = (1-\alpha)(dN/dS)$ . We computed these statistics for each species  
576 using the per branch dN/dS ratio, using either all mutations and substitutions, or only GC-  
577 conservative mutations and substitutions.

578 We used three different distributions to model the fitness effects of mutations that have been shown  
579 to perform the best in (18). Two of these models, GammaExpo and ScaledBeta, account for the  
580 existence of slightly beneficial non-synonymous mutations. We then averaged the estimates of the  
581 three models using Akaike weights as follows:

$$\overline{\alpha} = \alpha_{\text{GammaZero}} * \text{AICw}_{\text{GammaZero}} + \alpha_{\text{GammaExpo}} * \text{AICw}_{\text{GammaExpo}} + \alpha_{\text{ScaledBeta}} * \text{AICw}_{\text{ScaledBeta}}$$
$$\overline{\omega_a} = \omega_{\text{aGammaZero}} * \text{AICw}_{\text{GammaZero}} + \omega_{\text{aGammaExpo}} * \text{AICw}_{\text{GammaExpo}} + \omega_{\text{aScaledBeta}} * \text{AICw}_{\text{ScaledBeta}}$$
$$\overline{\omega_{na}} = \omega_{\text{naGammaZero}} * \text{AICw}_{\text{GammaZero}} + \omega_{\text{naGammaExpo}} * \text{AICw}_{\text{GammaExpo}} + \omega_{\text{naScaledBeta}} * \text{AICw}_{\text{ScaledBeta}}$$

582 where AICw stands for akaike weigths that were estimated using the akaike.weights fonction in R  
583 (<https://www.rdocumentation.org/packages/qpcR/versions/1.4-1/topics/akaike.weights>).

584 When estimating DFE model parameters, we accounted for recent demographic effects, as well as  
585 population structure and orientation errors, by using nuisance parameters, which correct each class  
586 of frequency of the synonymous and non-synonymous SFS relative to the neutral expectation in an  
587 equilibrium Wright–Fisher population (39).

588 We also estimated  $\alpha$ ,  $\omega_a$  and  $\omega_{na}$  at group level. Two approaches were used. Firstly, we pooled  
589 species specific SFS from each group, and used the dN/dS ratio of the total tree of each taxon. We  
590 did so following the unweighted and unbiased strategy of (34), which combines polymorphism data  
591 across species with equal weights. Briefly, we divided the synonymous and non-synonymous  
592 number of SNPs of each category of the SFS of each species by the total number of SNPs of the  
593 species, then we summed those normalized numbers across species and finally we transformed  
594 those sums so that the total number of SNPs of the pooled SFS matches the total number of SNPs  
595 across species. The resulting estimate was called  $\omega_{a[P]}$ . Secondly, we calculated the arithmetic mean  
596 of  $\omega_{na}$  across species within a taxonomic group to obtain a non-adaptive substitution rate at the  
597 group level. We then subtracted this average from the dN/dS ratio calculating across the whole tree  
598 of each taxon to obtain an estimate of the adaptive substitution rate at group level (called  $\omega_{a[A]}$ ).

599 **7. Life history traits variables**

600 Five life history traits were retrieved from the literature for each species: adult size (i.e. the average  
601 length of adults), body mass (i.e. the mean body mass of adults' wet weights), fecundity (i.e. the  
602 number of offspring released per day), longevity (i.e. the maximal recorded longevity in years), and  
603 propagule size (i.e. the size of the juvenile or egg or larva when leaving parents or group of  
604 relatives) (**Table S5**). In the case of social insects and birds, parental care is provided to juveniles  
605 until they reach adult size so in these cases, propagule size is equal to adult size.

606 **8. Simulations**

607 In order to evaluate whether our method to estimate the adaptive substitution rate could lead to a  
608 spurious correlation between  $\pi_s$  and  $\omega_a$ , we simulated the evolution of coding sequences in a single  
609 population undergoing demographic fluctuations using SLIM V2 (69). We considered panmictic  
610 populations of diploid individuals whose genomes consisted of 1500 coding sequences, each of 999  
611 base pairs. We set the mutation rate to 2.2e-9 per base pair per generation, the recombination rate to  
612 10e-8 per base (as in (23)) and the DFE to a gamma distribution of mean -740 and shape 0.14 for  
613 the negative part, and to an exponential distribution of mean  $10^{-4}$  for the positive part (those DFE  
614 parameters correspond to the DFE estimated from the pooled SFS of primates). We simulated  
615 several demographic scenarios with four regimes of frequency of the fluctuations, as well as four  
616 regimes of intensity of the fluctuations (see **figure S5**). We sampled polymorphism and divergence  
617 for 20 individuals at several time points during the simulations, evaluated  $\pi_s$  and  $\omega_a$  and measured  
618 the correlation between the two variables.

619 **Acknowledgments**

620 We thank Roger de Vila, Lise Dupont, Nicolas Bierne and Christophe Galkowski for providing us  
621 with tissue or DNA samples. We thank Iago Bonicci for the homemade program that allowed us to  
622 remove intronic sequences of the contigs obtained during the capture experiment by identifying any  
623 incongruent correspondence or inconsistent overlap on both the transcriptomic reference and the  
624 assembly of the capture experiment contigs. We also thank Yoann Anselmetti, Thibault Leroy and  
625 Jonathan Romiguier for their frequent help, Yoann Anciaux for sharing his experience with Fisher's

626 geometrical model predictions, and Thomas Bataillon for his pieces of advice with regards to the  
627 DFE- $\alpha$  method models and estimates.

628 **Data accessibility:**

629 Illumina raw reads of the capture experiment are deposited under the Bioproject PRJNA530965 in  
630 the SRA database.

631 **Conflict of interest disclosure:** The authors of this preprint declare that they have no financial  
632 conflict of interest with the content of this article. Nicolas Galtier is one of the PCI Evol Biol  
633 recommenders.

634 **Supplementary tables and figures legends:**

635 **Table S1 : Details of the species used in this study and numbers of individuals for each species.**

636 **Table S2 : Number of orthogroups for each taxonomic group.**

637 The differences in terms of number of orthogroups comes from the fact that we not only kept orthogroups with all  
638 species but also orthogroups with all species but one to estimate dN/dS value for each terminal branches in order to  
639 maximize the number of substitutions for data sets generated by exon capture.

640 **Table S3: SNPs counts for each species.**

641 SNPs counts are not integers because they corresponds to SNPs that are present in our SFS, where we chose a sample  
642 size (i.e. the number of categories of the SFS) lower than  $2*n$ , where  $n$  is the number of individuals. This is to  
643 compensate the uneven coverage between individuals that results in some sites in some individuals not to be genotyped.  
644 We chose sample sizes that maximize the number of SNPs in each SFS.

645 **Table S4: Sources of the tree topologies of each taxonomic group used to estimate branch  
646 length and map substitutions.**

647 **Table S5: Values and sources of the life history traits used in this study.**

648 **Tables S6 and S7: Per species and per group life history traits, polymorphism and divergence  
649 data,  $\alpha$ ,  $\omega_a$  and  $\omega_{na}$  estimates.**

650 **Figure S1: Cross contamination network for de novo assemblies from exon capture.**

651 Circles represent the assemblies, and arrows and their corresponding numbers represent the number of cross  
652 contaminants. Most cross contamination events occur between closely-related species and are therefore likely false  
653 positive cases.

654 **Figure S2: Relationship between  $\omega_{a[P]}$  and  $\pi_s$  and  $\log_{10}$  transformed life history traits.**

655  $\omega_{a[P]}$  is estimated using all mutations and substitutions (A) or using only GC-conservative mutations and substitutions  
656 (B). Group level  $\pi_s$  and life history traits are estimated by averaging species level estimates across closely related  
657 species. Black dotted lines represent significant regressions across taxonomic groups and grey dotted lines non-  
658 significant ones.

659 **Figure S3: Relationship between  $\omega_{a[A]}$  and  $\pi_s$  and  $\log_{10}$  transformed life history traits.**

660  $\omega_{a[A]}$  is estimated using all mutations and substitutions (A) or using only GC-conservative mutations and substitutions  
661 (B). Group level  $\pi_s$  and life history traits are estimated by averaging species level estimates across closely related  
662 species. Black dotted lines represent significant regressions across taxonomic groups and grey dotted lines non-  
663 significant ones.

664 **Figure S4: Relationship between species-level  $\omega_{na}$  and  $\pi_s$  and  $\log_{10}$  transformed life history  
665 traits.**

666  $\omega_{na}$  is estimated using all mutations and substitutions (A) or using only GC-conservative mutations and substitutions  
667 (B). Black dotted lines represent significant regressions across taxonomic groups and grey dotted lines non-significant  
668 ones.

669 **Figure S5: Relationship between species-level  $\alpha$  and  $\pi_s$ .**

670  $\alpha$  is estimated using all mutations and substitutions (A) or using only GC-conservative mutations and substitutions (B).  
671 The dotted line represents the regression across all species, and full lines represent the regression within each taxonomic  
672 groups. Black dotted lines represent significant regressions across taxonomic groups and grey dotted lines non-  
673 significant ones.

674 **Figure S6: Design of the simulations of fluctuation of population size.**

675 A: three fold ratio between low and high population size and high long-term population size.  
676 B: thirty fold ratio between low and high population size and high long-term population size.  
677 C: three fold ratio between low and high population size and low long-term population size.  
678 D: thirty fold ratio between low and high population size and low long-term population size.

679 **Figure S7: Relationship between  $\omega_a$  and  $\pi_s$  in simulated scenarios of fluctuating population  
680 size.**

681 A: three fold ratio between low and high population size and high long-term population size (scenario A in figure S1)  
682 B: thirty fold ratio between low and high population size and high long-term population size (scenario B in figure S1)  
683 C: three fold ratio between low and high population size and low long-term population size (scenario C in figure S1)  
684 D: thirty fold ratio between low and high population size and low long-term population size (scenario D in figure S1)

## 685 References:

1. Bell G. Evolutionary rescue and the limits of adaptation. *Philosophical Transactions of the Royal Society B: Biological Sciences*. 2013;368(1610):20120080.
2. Lanfear R, Kokko H, Eyre-Walker A. Population size and the rate of evolution. *Trends in Ecology & Evolution*. janv 2014;29(1):33-41.
3. Smith JM. What Determines the Rate of Evolution? *The American Naturalist*. 1 mai 1976;110(973):331-8.
4. Nam K, Munch K, Mailund T, Nater A, Greminger MP, Krützen M, et al. Evidence that the rate of strong selective sweeps increases with population size in the great apes. *Proceedings of the National Academy of Sciences*. 14 févr 2017;114(7):1613-8.
5. Bürger R, Lynch M. Evolution and extinction in a changing environment: a quantitative-genetic analysis. *Evolution*. 1995;49(1):151-63.
6. Barton N, Partridge L. Limits to natural selection. *BioEssays*. 2000;22(12):1075-84.
7. Kopp M, Hermisson J. The genetic basis of phenotypic adaptation II: the distribution of adaptive substitutions in the moving optimum model. *Genetics*. 2009;183(4):1453-76.
8. Karasov T, Messer PW, Petrov DA. Evidence that Adaptation in *Drosophila* Is Not Limited by Mutation at Single Sites. *PLOS Genetics*. 17 juin 2010;6(6):e1000924.
9. Weissman DB, Barton NH. Limits to the Rate of Adaptive Substitution in Sexual Populations. *PLOS Genetics*. 7 juin 2012;8(6):e1002740.
10. Yeaman S, Gerstein AC, Hodgins KA, Whitlock MC. Quantifying how constraints limit the diversity of viable routes to adaptation. *PLoS genetics*. 2018;14(10):e1007717.
11. Huber CD, Kim BY, Marsden CD, Lohmueller KE. Determining the factors driving selective effects of new nonsynonymous mutations. *Proceedings of the National Academy of Sciences*. 2017;114(17):4465-70.
12. McDonald JH, Kreitman M. Adaptive protein evolution at the *Adh* locus in *Drosophila*. *Nature*. 20 juin 1991;351(6328):652-4.
13. Smith NGC, Eyre-Walker A. Adaptive protein evolution in *Drosophila*. *Nature*. févr 2002;415(6875):1022-4.
14. Keightley PD, Eyre-Walker A. Joint inference of the distribution of fitness effects of deleterious mutations and population demography based on nucleotide polymorphism frequencies. *Genetics*. 2007;177(4):2251-61.
15. Boyko AR, Williamson SH, Indap AR, Degenhardt JD, Hernandez RD, Lohmueller KE, et al. Assessing the evolutionary impact of amino acid mutations in the human genome. *PLoS genetics*. 2008;4(5):e1000083.

16. Eyre-Walker A, Keightley PD. Estimating the Rate of Adaptive Molecular Evolution in the Presence of Slightly deleterious Mutations and Population Size Change. *Mol Biol Evol*. 1 sept 2009;26(9):2097-108.
17. Messer PW, Petrov DA. Frequent adaptation and the McDonald–Kreitman test. *PNAS*. 21 mai 2013;110(21):8615-20.
18. Galtier N. Adaptive Protein Evolution in Animals and the Effective Population Size Hypothesis. *PLOS Genetics*. 11 janv 2016;12(1):e1005774.
19. Keightley PD, Campos JL, Booker TR, Charlesworth B. Inferring the Frequency Spectrum of Derived Variants to Quantify Adaptive Molecular Evolution in Protein-Coding Genes of *Drosophila melanogaster*. *Genetics*. 1 juin 2016;203(2):975-84.
20. Tataru P, Mollion M, Glémin S, Bataillon T. Inference of Distribution of Fitness Effects and Proportion of Adaptive Substitutions from Polymorphism Data. *Genetics*. 1 nov 2017;207(3):1103-19.
21. Loewe L, Charlesworth B. Inferring the distribution of mutational effects on fitness in *Drosophila*. *Biology Letters*. 22 sept 2006;2(3):426-30.
22. Stoletzki N, Eyre-Walker A. Estimation of the neutrality index. *Molecular biology and evolution*. 2010;28(1):63-70.
23. Rousselle M, Mollion M, Nabholz B, Bataillon T, Galtier N. Overestimation of the adaptive substitution rate in fluctuating populations. *Biology Letters*. 1 mai 2018;14(5):20180055.
24. Eyre-Walker A. Changing effective population size and the McDonald-Kreitman test. *Genetics*. 2002;162(4):2017-24.
25. Corcoran P, Gossmann TI, Barton HJ, Slate J, Zeng K. Determinants of the Efficacy of Natural Selection on Coding and Noncoding Variability in Two Passerine Species. *Genome Biol Evol*. 1 nov 2017;9(11):2987-3007.
26. Rousselle M, Laverré A, Figuet E, Nabholz B, Galtier N. Influence of Recombination and GC-biased Gene Conversion on the Adaptive and Nonadaptive Substitution Rate in Mammals versus Birds. *Mol Biol Evol [Internet]*. [cité 22 févr 2019]; Disponible sur: <https://academic.oup.com/mbe/advance-article/doi/10.1093/molbev/msy243/5261349>
27. Bolívar P, Mugal CF, Rossi M, Nater A, Wang M, Dutoit L, et al. Biased inference of selection due to GC-biased gene conversion and the rate of protein evolution in flycatchers when accounting for it. *Mol Biol Evol [Internet]*. [cité 3 août 2018]; Disponible sur: <https://academic.oup.com/mbe/advance-article/doi/10.1093/molbev/msy149/5063898>
28. Ohta T. The Nearly Neutral Theory of Molecular Evolution. *Annual Review of Ecology and Systematics*. 1992;23(1):263-86.
29. Gossmann TI, Keightley PD, Eyre-Walker A. The Effect of Variation in the Effective Population Size on the Rate of Adaptive Molecular Evolution in Eukaryotes. *Genome Biol Evol*. 1 janv 2012;4(5):658-67.

30. Gossman TI, Song B-H, Windsor AJ, Mitchell-Olds T, Dixon CJ, Kapralov MV, et al. Genome wide analyses reveal little evidence for adaptive evolution in many plant species. *Molecular biology and evolution*. 2010;27(8):1822-32.
31. Strasburg JL, Kane NC, Raduski AR, Bonin A, Michelmore R, Rieseberg LH. Effective population size is positively correlated with levels of adaptive divergence among annual sunflowers. *Molecular biology and evolution*. 2010;28(5):1569-80.
32. Lourenço JM, Glémin S, Galtier N. The rate of molecular adaptation in a changing environment. *Molecular biology and evolution*. 2013;30(6):1292-301.
33. Simion P, Belkhir K, François C, Veyssier J, Rink JC, Manuel M, et al. A software tool ‘CroCo’ detects pervasive cross-species contamination in next generation sequencing data. *BMC biology*. 2018;16(1):28.
34. James JE, Piganeau G, Eyre-Walker A. The rate of adaptive evolution in animal mitochondria. *Molecular ecology*. 2016;25(1):67-78.
35. Galtier N, Roux C, Rousselle M, Romiguier J, Figuet E, Glémin S, et al. Codon Usage Bias in Animals: Disentangling the Effects of Natural Selection, Effective Population Size, and GC-Biased Gene Conversion. *Molecular biology and evolution*. 2018;35(5):1092-103.
36. Romiguier J, Gayral P, Ballenghien M, Bernard A, Cahais V, Chenuil A, et al. Comparative population genomics in animals uncovers the determinants of genetic diversity. *Nature*. 2014;515(7526):261.
37. Chen J, Glémin S, Lascoux M. Genetic Diversity and the Efficacy of Purifying Selection across Plant and Animal Species. *Molecular Biology and Evolution*. juin 2017;34(6):1417-28.
38. Zhen Y, Huber CD, Davies RW, Lohmueller KE. Stronger and higher proportion of beneficial amino acid changing mutations in humans compared to mice and flies. 26 sept 2018 [cité 10 oct 2018]; Disponible sur: <http://biorxiv.org/lookup/doi/10.1101/427583>
39. Eyre-Walker A, Woolfit M, Phelps T. The Distribution of Fitness Effects of New Deleterious Amino Acid Mutations in Humans. *Genetics*. 1 juin 2006;173(2):891-900.
40. Jensen JD, Bachtrog D. Characterizing the Influence of Effective Population Size on the Rate of Adaptation: Gillespie’s Darwin Domain. *Genome Biol Evol*. 24 juin 2011;3:687-701.
41. Gillespie JH. IS THE POPULATION SIZE OF A SPECIES RELEVANT TO ITS EVOLUTION? - Gillespie - 2001 - Evolution - Wiley Online Library [Internet]. 2001 [cité 11 juill 2019]. Disponible sur: <https://onlinelibrary.wiley.com/doi/abs/10.1111/j.0014-3820.2001.tb00732.x>
42. Gillespie JH. The neutral theory in an infinite population. *Gene*. 2000;261(1):11-8.
43. Corbett-Detig RB, Hartl DL, Sackton TB. Natural Selection Constrains Neutral Diversity across A Wide Range of Species. *PLOS Biology*. 10 avr 2015;13(4):e1002112.

44. Coop G. Does linked selection explain the narrow range of genetic diversity across species? *bioRxiv*. 7 mars 2016;042598.
45. Enard D, Cai L, Gwennap C, Petrov DA. Viruses are a dominant driver of protein adaptation in mammals. :25.
46. Razeto-Barry P, Díaz J, Vásquez RA. The nearly neutral and selection theories of molecular evolution under the fisher geometrical framework: substitution rate, population size, and complexity. *Genetics*. 2012;191(2):523-34.
47. Orr HA. Adaptation and the Cost of Complexity. *Evolution*. 1 févr 2000;54(1):13-20.
48. Valentine JW, Collins AG, Meyer CP. Morphological complexity increase in metazoans. *Paleobiology*. 1994;20(2):131-42.
49. Stumpf MP, Thorne T, de Silva E, Stewart R, An HJ, Lappe M, et al. Estimating the size of the human interactome. *Proceedings of the National Academy of Sciences*. 2008;105(19):6959-64.
50. Fernández A, Lynch M. Non-adaptive origins of interactome complexity. *Nature*. 2011;474(7352):502.
51. Rousselle M, Faivre N, Ballenghien M, Galtier N, Nabholz B. Hemizygosity Enhances Purifying Selection: Lack of Fast-Z Evolution in Two Satyrine Butterflies. *Genome Biol Evol*. 1 oct 2016;8(10):3108-19.
52. Ballenghien M, Faivre N, Galtier N. Patterns of cross-contamination in a multispecies population genomic project: detection, quantification, impact, and solutions. *BMC Biology [Internet]*. déc 2017 [cité 12 mars 2018];15(1). Disponible sur: <http://bmcbiol.biomedcentral.com/articles/10.1186/s12915-017-0366-6>
53. Meyer M, Kircher M. Illumina sequencing library preparation for highly multiplexed target capture and sequencing. *Cold Spring Harbor Protocols*. 2010;2010(6):pdb. prot5448.
54. Tilak M-K, Justy F, Debiais-Thibaud M, Botero-Castro F, Delsuc F, Douzery EJP. A cost-effective straightforward protocol for shotgun Illumina libraries designed to assemble complete mitogenomes from non-model species. *Conservation Genet Resour*. 1 mars 2015;7(1):37-40.
55. Rohland N, Reich D. Cost-effective, high-throughput DNA sequencing libraries for multiplexed target capture. *Genome research*. 2012;
56. Bolger AM, Lohse M, Usadel B. Trimmomatic: a flexible trimmer for Illumina sequence data. *Bioinformatics*. 2014;30(15):2114-20.
57. Cahais V, Gayral P, Tsagkogeorga G, Melo-Ferreira J, Ballenghien M, Weinert L, et al. Reference-free transcriptome assembly in non-model animals from next-generation sequencing data. *Molecular ecology resources*. 2012;12(5):834-45.
58. Simpson JT, Wong K, Jackman SD, Schein JE, Jones SJ, Birol I. ABySS: a parallel assembler for short read sequence data. *Genome research*. 2009;19(6):1117-23.

59. Huang X, Madan A. CAP3: A DNA sequence assembly program. *Genome research*. 1999;9(9):868-77.
60. Grabherr MG, Haas BJ, Yassour M, Levin JZ, Thompson DA, Amit I, et al. Full-length transcriptome assembly from RNA-Seq data without a reference genome. *Nature biotechnology*. 2011;29(7):644.
61. Li H, Durbin R. Fast and accurate short read alignment with Burrows–Wheeler transform. *Bioinformatics*. 2009;25(14):1754-60.
62. Tsagkogeorga G, Cahais V, Galtier N. The population genomics of a fast evolver: high levels of diversity, functional constraint, and molecular adaptation in the tunicate *Ciona intestinalis*. *Genome Biology and Evolution*. 2012;4(8):852-61.
63. Gayral P, Melo-Ferreira J, Glémén S, Bierne N, Carneiro M, Nabholz B, et al. Reference-free population genomics from next-generation transcriptome data and the vertebrate–invertebrate gap. *PLoS genetics*. 2013;9(4):e1003457.
64. Ranwez V, Delsuc F, Ranwez S, Belkhir K, Tilak M-K, Douzery EJ. OrthoMaM: a database of orthologous genomic markers for placental mammal phylogenetics. *BMC evolutionary biology*. 2007;7(1):241.
65. Douzery EJ, Scornavacca C, Romiguier J, Belkhir K, Galtier N, Delsuc F, et al. OrthoMaM v8: a database of orthologous exons and coding sequences for comparative genomics in mammals. *Molecular biology and evolution*. 2014;31(7):1923-8.
66. Emms DM, Kelly S. OrthoFinder: solving fundamental biases in whole genome comparisons dramatically improves orthogroup inference accuracy. *Genome biology*. 2015;16(1):157.
67. Ranwez V, Harispe S, Delsuc F, Douzery EJ. MACSE: Multiple Alignment of Coding SEquences accounting for frameshifts and stop codons. *PloS one*. 2011;6(9):e22594.
68. Guéguen L, Gaillard S, Boussau B, Gouy M, Groussin M, Rochette NC, et al. Bio++: efficient extensible libraries and tools for computational molecular evolution. *Molecular biology and evolution*. 2013;30(8):1745-50.
69. Haller BC, Messer PW. SLiM 2: Flexible, Interactive Forward Genetic Simulations. *Mol Biol Evol*. 1 janv 2017;34(1):230-40.